Personal Computer Programs To Generate Reference Diffraction Patterns

J. T. Staley

Alcoa Technical Center, Alcoa Center, Pennsylvania 15069

Received June 4, 1992

Interrogating crystalline materials with beams of electrons or X-radiation provides valuable information to chemists, physicists, and material scientists regarding the nature of the material. Materials can be identified by comparing their electron or X-ray diffraction patterns with those of known materials. For both Debye–Scherrer X-ray powder patterns and electron diffraction patterns, both paper and computer files exist which aid interpretation. Comparing patterns generated using a personal computer from theoretical models with patterns of unknowns is a newer method to assist in identification. This paper describes two computer programs, DIFPAT and POWDER, which simulate electron diffraction and Debye–Scherrer powder patterns. They are available for both IBM-compatible and Macintosh computers. Patterns for candidate unknowns can be displayed on the screen in seconds from the database, which contains about 100 of the most common structures. In addition, the users may input the atomic positions and crystal parameters for any candidate structure and build their own database. The patterns may also be printed to scale using a laser printer.

INTRODUCTION

One way to characterize and identify crystalline materials is to interpret patterns that arise when a wave of electrons or X-rays is diffracted by the atom planes in the crystal. This paper describes user-friendly software which rapidly produces reference diffraction patterns for comparison with unknowns. Two programs are described: DIFPAT simulates electron diffraction patterns, while POWDER simulates X-ray powder diffraction patterns.

DIFPAT

An electron diffraction pattern is a map of the intensity of electrons scattered from a beam of electrons by the atom planes in a crystal. In conventional transmission electron microscopy, the objective lens focuses the scattered electrons in the back focal plane, and a diffraction pattern is visible if this plane is imaged. Many factors influence the form of a diffraction pattern. When a beam of electrons interacts with a crystal, strongly diffracted beams arise in directions which depend on the orientation and structure of the crystal. The intensity of these diffracted beams is a function of the scattering factor of the atoms composing the crystal, the symmetry of the crystal, and the distance of the beams from the transmitted beam. The information in a diffraction pattern is used to determine the crystal system and lattice type, the orientation of the crystal, and the Miller indices of crystal planes that satisfy a specific scattering law. Because the properties of materials depend on their structure, almost every materials research facility has a need to interpret diffraction patterns.

Interpreting many of these patterns, particularly patterns of intermetallic compounds, is difficult and time consuming. Simulated electron diffraction patterns are used as an aid in visualizing how orientation and atomic structure affect the distribution of spots in real patterns. Edington[1] and Loretto,[2] for example, give several examples of simulations of diffraction patterns for face-centered and body-centered cubic crystal crystals and for close-packed hexagonal structures having an ideal c/a ratio where c and a are the lengths of the unit cell of the crystal.

There are a myriad number of combinations of crystal structures and zone axes (i.e., nonequivalent planes of a crystal sharing a common crystallographic direction). Consequently, no book provides examples for even a small fraction of all possible diffraction patterns. Moreover, intensity differences, except for examples of superlattice reflections such as found in $AuCu_3$, are rarely simulated in text figures. Mainframe computer programs to simulate electron diffraction patterns have been available in certain universities, but they are usually not transportable. Moreover, they are generally not user-friendly, nor do they provide interactive graphics. The power and availability of the personal computer, however, now makes it possible to overcome these limitations.

This paper describes a menu-driven program for personal computers which uses interactive graphics to simulate single-crystal electron diffraction patterns. A pattern is modeled assuming the interaction of a parallel beam of electrons with a thin, perfect single crystal. Effects of the scattering factor of atomic species on the diffracting planes and of deviation from the Bragg angle are included, and simulating the effect of double diffraction is an option. Effects such as twinning and multiple patterns arising in two-phase samples are also considered. Because of the importance of the crystal structure on the diffraction pattern, the computer program models the crystal structure as well as the diffraction pattern. Thus, effects of crystal symmetry and chemical composition on the intensity of the simulated pattern can be more readily visualized. The axes of the crystal model are scaled, and the atoms are presented as spheres which are small relative to the cell dimensions, so that the symmetry can be recognized easily. To aid in visualization, the crystal model can be rotated along different axes. The crystal model and diffraction simulation can be plotted to high resolution using either a dot matrix printer or a laser printer.

Program Overview. The program uses pull-down menus [accessed by the function keys for the IBM-compatible (DOS) version and by the mouse for the Macintosh (Mac) version]. The user inputs crystal parameters, atom locations, and atomic species either by selecting from the menus provided, by entering from the keyboard, or by retrieving data previously entered from the keyboard. Selection is based on crystal structure, Bravais lattice, Strukturbericht, Pearson symbol, structure prototype, and space group. Almost 100 of the structures that are the most widely examined by materials scientists are provided. An example of the menu system on a DOS computer is illustrated in Figure 1. For the case of crystals selected

0095-2338/93/1633-0059$04.00/0 © 1993 American Chemical Society

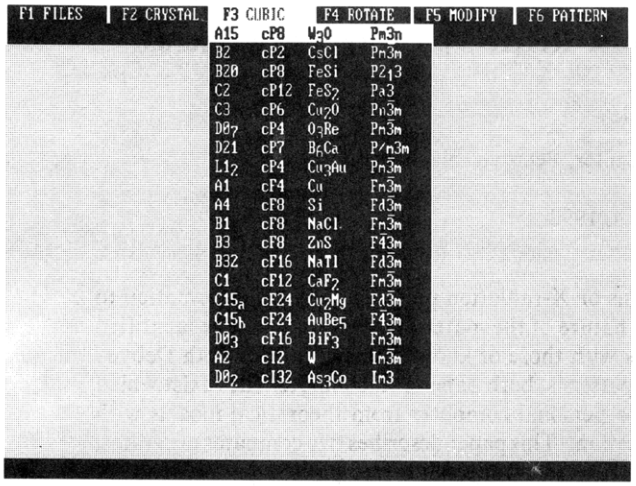

Figure 1. Menu screen on DOS computer.

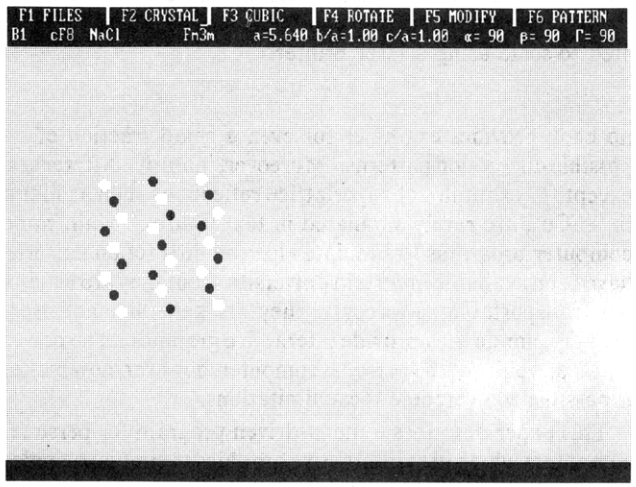

Figure 2. DOS screen print showing crystal model of unit cell of NaCl.

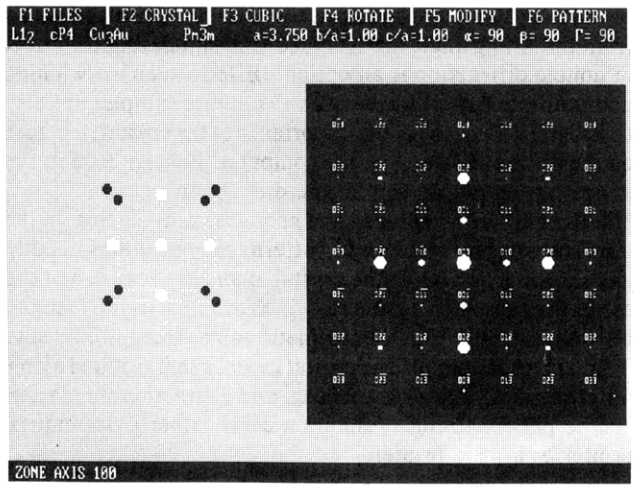

Figure 3. DOS screen print showing [100] diffraction pattern for Cu_3Au.

from the menu, the user is given the opportunity to modify atomic species and crystal parameters. After the crystal data have been established, an open model of the crystal is displayed. A DOS screen print of a model of NaCl is presented in Figure 2. The model can be rotated around the axes in real time to aid in visualization of the atomic arrangements. After the zone axis is input, an annotated representation of the diffraction pattern is displayed as illustrated in Figure 3 for a DOS screen. In addition, the crystal model is reoriented so that the zone axis parallels that of the diffraction pattern. In this way, the relationship between crystal symmetry and the distribution and intensity of spots is most readily seen. At this point in the program, the user can have the program test for and display spots that could be visible by effects of double diffraction or from twinning on planes perpendicular to the zone axis. (Twinning is a shift in atom planes resulting in the creation of a mirror plane in the lattice that possesses no translational symmetry.) The double diffraction spots for the ⟨110⟩ zone axis of Si is illustrated on the screen print of a Mac, Figure 4. A table can also be displayed which gives the angles and distances of the major spots relative to the central spot. Furthermore, patterns can be overlaid on the screen. In this way, a representation of precipitates in a matrix can be obtained. This feature is illustrated in Figure 5, a Mac screen print of the ⟨0001⟩ pattern of $MgZn_2$ overlaid on the ⟨111⟩ pattern of Cu.

A laser printer can be used to provide high-resolution hard copies, or dot matrix printers can be used. The size of the patterns can be modified on the printed output so that patterns can be matched with those on film. Plots of the DOS version simulation of the patterns for Si crystals using a zone axis of ⟨110⟩ are presented in Figure 6. After displaying and optionally plotting the patterns, the user is given the opportunity to select another zone axis, modify the camera constant of the display, or select another crystal.

The most calculation-intense portions of the program are those which simulate the diffraction pattern. These include routines that (1) determine which planes cause diffraction, (2) determine the spatial relationship of the beams relative to the transmitted beam and convert this information into x, y coordinates of the spots, and (3) calculate the intensities of the diffracted beams. The portions of the program which convert the crystal parameters into x, y coordinates to display the crystal model also require a large number of calculations. The mathematical basis for the diffraction theory and the concept of a reciprocal lattice in addition to the crystal lattice will be discussed. Enough of this theory will be reviewed so that the nature of the calculations required can be described.

Determining Orientation and Identity of Spots. Each spot in an electron diffraction pattern arises from a beam of electrons diffracted from a particular set of atomic planes in the crystal. The pattern of spots represents a planar section of the reciprocal lattice. The direction of the electron beam relative to the crystal, known as the zone axis, determines which section is imaged. The reciprocal lattice can be described as follows. Let **a**, **b**, and **c** equal the base vectors of a crystal lattice so that the vector to any lattice point is given by $p = u\mathbf{a} + v\mathbf{b} + w\mathbf{c}$ where u, v, and w are Miller indices of directions in the crystal. The definition of the vectors which define the reciprocal lattice is that the translations $\mathbf{a}^*a = \mathbf{b}^*b = \mathbf{c}^*c = 1$. The absolute value of $\mathbf{a}^* = 1/a$, where a equals the a-spacing of the crystal lattice, and similar relationships hold for $\mathbf{b}^*$ and $\mathbf{c}^*$. The vector defined by $\mathbf{g}^* = h\mathbf{a}^* + k\mathbf{b}^* + l\mathbf{c}^*$ is normal to the plane of Miller indices (h,k,l) in the crystal lattice. The magnitude of this vector is the reciprocal of the spacing of (h,k,l) in the crystal lattice.

The conditions which give rise to diffraction are defined by the well-known Bragg equation:

$$\lambda = 2d \sin(\theta) \qquad (1)$$

where λ is the wavelength of the electrons, d is the interplanar spacing of the diffracting planes, and 2θ is the angle between the incident beam of electrons and the beam diffracted by those planes. This phenomenon is illustrated by the Ewald

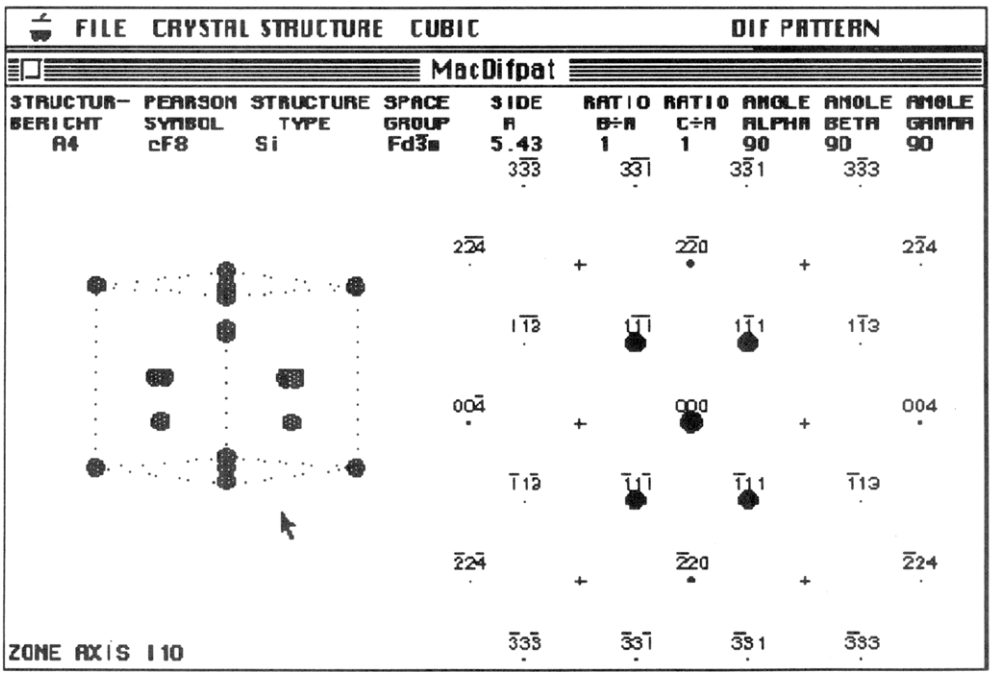

Figure 4. Mac screen print showing [110] electron diffraction pattern of silicon.

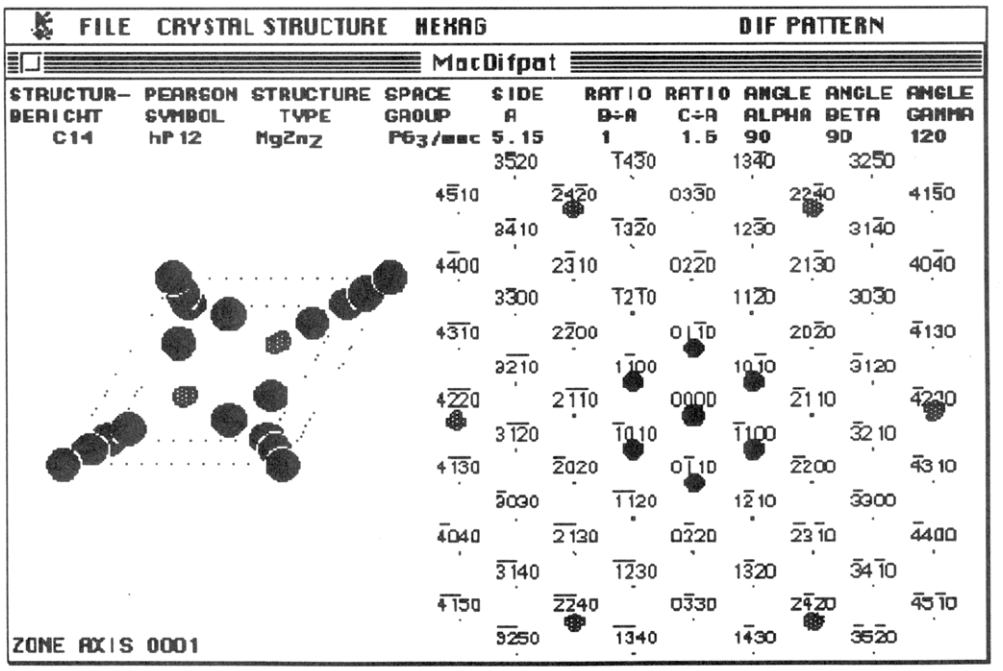

Figure 5. Mac screen print of [111] diffraction pattern of Cu overlaid on [0001] pattern for $MgZn_2$.

sphere construction in Figure 7. Diffraction occurs on those planes which intersect the Ewald sphere. Because λ is small (<0.004 nm for 100 kV electrons), the angle θ is about one-half degree for low index planes. Hence, planes giving rise to strong maxima are almost parallel to the electron beam direction. Moreover, the diffraction maxima will be points only when the crystal is infinitely thick. For the case of typical thin specimens, the diffraction maxima extend parallel to the beam direction and assume a rod shape in reciprocal space (rel-rod). Therefore, the Ewald sphere can intersect these rods even when the incident beam does not satisfy the Bragg equation exactly. As a result of this effect and the small angle of incidence, a large number of planes will be sufficiently close to their Bragg angles to give rise to a large number of diffracted beams when the beam is parallel to an important zone axis. These beams give rise to the spots in the pattern. Because the radius of the Ewald sphere is inversely proportional to the wavelength of the electron, it is about 100 times larger than the spacing of the reciprocal lattice. The diffraction maxima are rel-rods, and the diffraction pattern represents a planar section through the origin of the reciprocal lattice. The zone axis is normal to all of the planes on this planar section. Consequently, the dot product of the vectors defining planes on this section and the vector defining the zone axis equal zero. This relationship is used in the computer program to determine which planes diffract. For a particular zone axis, the distances of the spots from the central spot arising from the transmitted beam and the orientation of these spots relative to each other depend on the crystal system and the interplanar distances. The distance of any spot from the central spot is proportional to the reciprocal lattice spacing and, hence, to the reciprocal of the interplanar spacing of the crystal. The angle between spots is related to angles between planes in the reciprocal lattice and, therefore, related to angles between

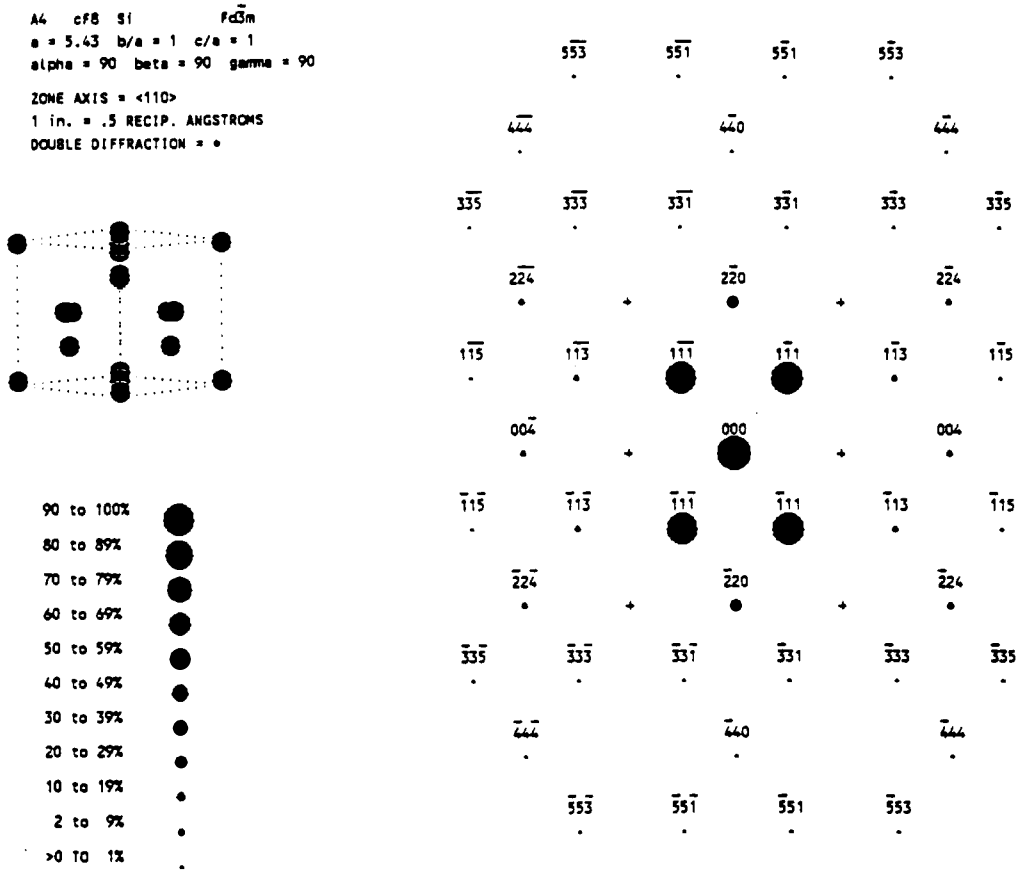

Figure 6. Laser printer output of [110] zone axis electron diffraction pattern of Si.

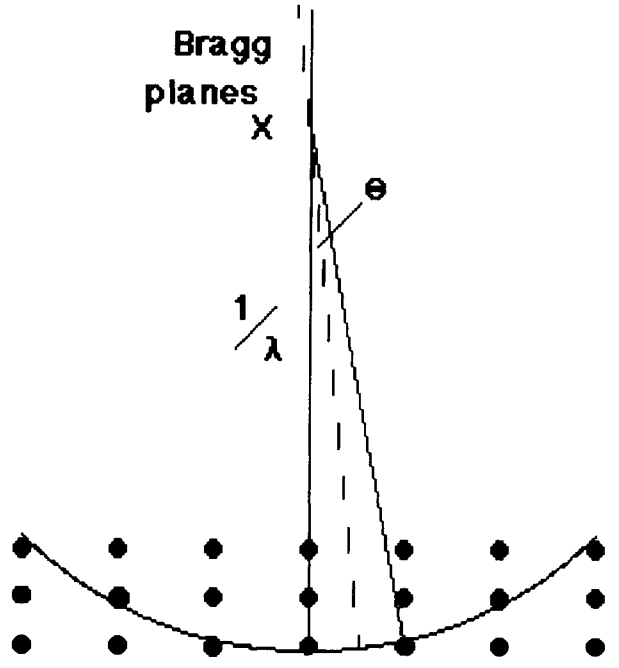

Figure 7. Schematic diagram showing Ewald sphere construction.

planes in the crystal. The equations given by Loretto[2] were used to determine the interplanar spacing and angles of the crystals. Because the vectors that define the reciprocal lattice may not be orthogonal or equal in length, some relationship between real space vectors and reciprocal lattice vectors must be established to allow translation from one coordinate system to another to simulate the pattern. The matrices along with the accompanying formulas in Table I taken from Sirotin and Shaskolskaya[3] describe this relationship for primitive lattices. These formulas and matrices are used in the computer program to transform reciprocal lattice points to x, y coordinates for display on the screen and for plotting.

Table I. Transformation Matrix for Reciprocal Lattice

	Triclinic[a]	
$a^*\sigma/\sin\sigma\sin\beta$	0	$-c^*\sigma/\tan\beta\sin\gamma$
$a^*\cos\gamma^*$	b^*	$c^*\cos\alpha^*$
0	0	$c^*\alpha\sin\gamma$
	Monoclinic[b]	
a^*	0	$c^*\cos\beta$
0	b^*	0
0	0	$c^*\sin\beta$
	Orthorhombic[c]	
a^*	0	0
0	b^*	0
0	0	c^*
	Tetragonal[d]	
a^*	0	0
0	b^*	0
0	0	c^*
	Hexagonal[e]	
$a^*\sqrt{3/2}$	0	
$a^*\sqrt{2}$	a^*	0
0	0	c^*
	Cubic[f]	
a^*	0	0
0	a^*	0
0	0	a^*

[a] $\sigma = \sqrt{1 - \cos^2\alpha - \cos^2\beta - \cos^2\gamma + 2\cos\alpha\cos\beta\cos\gamma}$; $a^* = \sin\alpha/a\sigma$; $b^* = \sin\beta/b\sigma$; $c^* = \sin\gamma/c\sigma$; $\cos\alpha^* = (\cos\beta\cos\gamma - \cos\alpha)/\sin\beta\sin\gamma$; $\cos\gamma^* = (\cos\alpha\cos\beta - \cos\gamma)/\sin\alpha\sin\beta$. [b] $a^* = 1/(a\sin\beta)$; $b^* = 1/b$; $c^* = 1(/c\sin\beta)$. [c] $a^* = 1/a$; $b^* = 1/b$; $c^* = 1/c$. [d] $a^* = 1/a$; $b^* = 1/a$; $c^* = 1/c$. [e] $a^* = b^* = 2/(a\sqrt{3})$; $c^* = 1/c$. [f] $a^* = 1/a$.

Calculating Beam Intensities. The intensities of the diffracted beams depend on the atomic scattering potentials of the species involved and the crystal symmetry. They are

proportional to the square of the scattering factor. The kinematical structure factor for reflections can be expressed as follows:

$$|F_{hkl}|^2 = \sum f_n \exp[-2\pi i(hx_n ky_n + lz_n)] \quad (2)$$

where h, k, and l are Miller indices of the planes and f_n, x_n, y_n, and z_n are scattering factors and coordinates of the atoms in the unit cell, respectively. Values of x_n, y_n, and z_n are expressed as fractions of the unit distances along u, v, and w.

For primitive lattices containing only one atom at 0, 0, 0, the structure factor is independent of h, k, and l, and reflections from all planes will be present. For other cases, application of eq 2 will reveal that destructive interference can cause certain reflections to be absent. This form of the equation using the square root of −1 is especially suited for examining simple systems because inspection can be used to determine which reflections are forbidden (have zero intensity). For example, the diffracted intensity would be zero in a body-centered cubic Bravais lattice when $(h + k + l)$ are odd and in a face-centered cubic Bravais lattice when h, k, and l are mixed.

Although eq 2 is simple, imaginary numbers are difficult to handle in a program. A trigonometric form of this equation avoids this complication:[7]

$$|F_{hkl}|^2 = \sum f_n (\cos^2 [2\pi(hx_n + ky_n + lz_n)] + \sin^2 [2\pi(hx_n + ky_n + lz_n)]) \quad (3)$$

This form of the structure factor equation was used in the computer program to calculate relative intensities because it avoids imaginary numbers. It easily calculates forbidden reflections as well as the intensities for those cases where symmetry is decreased because some of the atoms were replaced by atoms of another species in particular sites.

The extent of deviation from the Bragg angle also influences the intensity of the diffracted beams because the cross section of the rel-rod intercepted by the Ewald sphere decreases with increasing distance from the transmitted beam. Consequently, intensity of the diffracted beams decreases with distance from the central spot. The magnitude of the decrease depends on the scattering factor of the atomic species. This phenomenon was modeled by fitting equations to the data given in Appendix 8 in Edington.[1] Different spot diameters were used in the simulations to represent the effect of beam intensities on the appearance of the spots in a diffraction pattern.

Crystal Model. The crystal is described by the relative lengths and angles between the basis vectors and the locations of the atoms in the unit cell relative to these vectors. In general, the coordinate system describing the crystal is not orthogonal. To model the crystal, the data must be transformed so that it can be described in Cartesian x, y, z coordinates. The transformation matrix in Table II taken from Sirotin and Shaskolskaya[3] performs this function. To display the three-dimensional model on a two-dimensional screen, the y coordinate was ignored, and data representing the corners of the unit cell and the atom positions were displayed using the painter's algorithm similar to that used by Kirkland to display models of molecules.[4] That is, the data were sorted using a Shell sort[5] so that the points furthest from the viewer were at the top of the array. Then the points were displayed so that the points nearest the viewer overlaid those further away. To rotate the crystal about the z axis, and to provide a perspective view when the crystal model was displayed and plotted normal to the zone axis, the axes were transformed according to the transfomation matrix in Table III taken from Park.[6]

Table II. Transformation Matrix for Crystal Coordinates[a]

Triclinic		
$a \sin \beta$	0	$a \cos \beta$
$-b \sin \alpha \cos \gamma^*$	$b\sigma/\sin \beta$	$b \cos \alpha$
0	0	c
Monoclinic		
$a \sin \beta$	0	$a \cos \beta$
0	b	0
0	0	c
Orthorhombic		
a	0	0
0	b	0
0	0	c
Tetragonal		
a	0	0
0	a	0
0	0	c
Hexagonal		
$a^*\sqrt{3/2}$	0	0
$a^*\sqrt{2}$	a	0
0	0	c^*
Cubic		
a	0	0
0	a	0
0	0	a

[a] $\sigma = \sqrt{1 - \cos^2 \alpha - \cos^2 \beta - \cos^2 \gamma + 2 \cos \alpha \cos \beta \cos \gamma}$; $\cos \gamma^* = (\cos \alpha \cos \beta - \cos \gamma)/\sin \alpha \sin \beta$.

Table III. Matrix To Transform and Rotate Crystal Model Coordinates

$\cos \phi$	$\sin \phi$	0	0
$-\sin \phi \cos \theta$	$\cos \phi \cos \theta$	$\sin \theta$	0
$-\sin \phi \sin \theta$	$-\cos \phi \sin \theta$	$-\cos \phi$	0
0	0	0	1

Hardware Required. The DOS version of the program will run on any personal computer utilizing either an EGA or VGA graphics adapter. A color monitor is not required but adds to the program. A Hewlett–Packard-compatible laser printer or an Epson or compatible dot matrix printer is needed to plot the pattern. The Mac version will run on any Macintosh. A color monitor and card is suggested but is not needed.

POWDER

Principles. X-ray diffraction techniques are very useful in the characterization of crystallization materials. In particular, X-ray powder diffraction is widely used to identify the phases present in a variety of materials. For chemical phase identification and quantitative analysis of mixtures, this technique typically uses a sample that is composed of a powder of many small crystallites, <40 μm. In the basis setup, the sample is interrogated by a collimated monochromatic beam. If the powder particle is oriented to satisfy the Bragg angle, it will diffract the beam. The net result is that the resulting assemblage of diffracted beams from the powder sample approximates that which would result if a single crystal of each phase present in the sample were presented at all possible angles to the incident beam. Therefore, many coaxial cones of radiation emanate from the sample. The location and intensity of these cones may be detected using either film or an electronic detector. Several combinations of sample form, detector, and geometry are used regularly, and many special setups may be employed depending on the goal of the

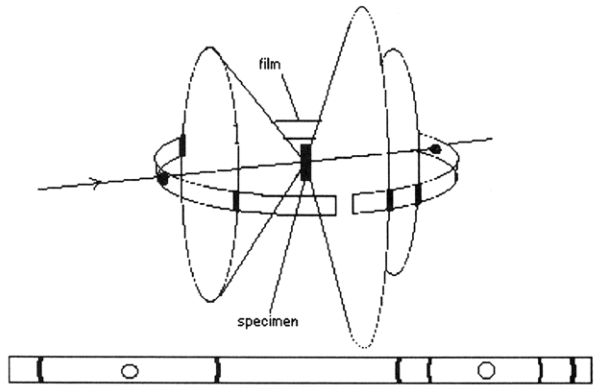

Figure 8. Schematic of Debye–Scherrer powder diffraction method.

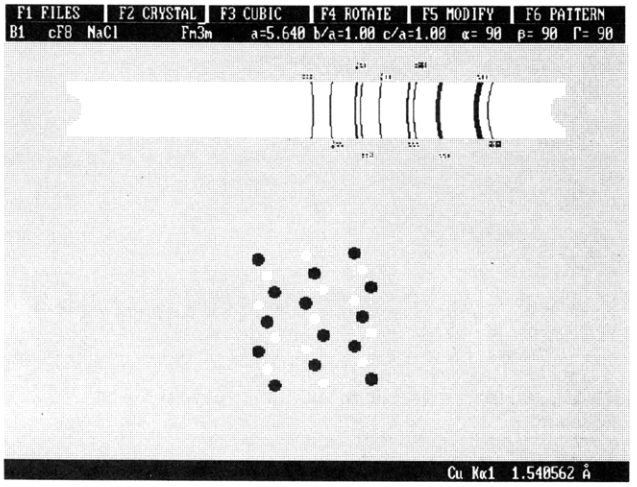

Figure 9. DOS screen print showing diffraction pattern of NaCl.

experiment. When the phase is present in a metal alloy, the sample is usually a thin foil. For these samples, each grain and each second-phase particle behaves like a single crystal. When the crystallographic texture of the sample is random, the intensities of the cones of radiation are similar to those from a powder sample. When the texture is nonrandom, however, the intensities depend on the nature of the texture.

Experimental Methods. Two widely employed methods which use film to detect the diffracted radiation are the Debye–Scherrer and Guinier. All of the diffracted beams are detected simultaneously by a cylinder of film which surrounds the sample, Figure 8. In the Debye–Scherrer method, the sample is typically powder. In the Guinier method, which is used to a large extent by metallurgists, the sample is a metal foil. A focusing crystal monochromator and a focusing camera provide higher resolution in the Guinier method. The pattern made on the film by the diffracted cones of radiation is characterized by the positions of the resulting lines on the film and on the degree of darkening or intensity of each line. The angular position, Θ, on the film depends on the spacing, d, of the planes of atoms which cause diffraction and on the wavelength, λ, of the incident x-radiation:

$$\lambda = 2d \sin \Theta \qquad (4)$$

The intensity of the lines depends on the atomic species and the arrangement of atoms in the unit cell of the crystal.

Phase Identification. Phases are identified by matching the patterns with those of known phases. For single-phase materials this is usually straightforward. For those materials containing multiple phases, phase identification can be difficult because of the intermingling of the lines. The database maintained by International Centre for Diffraction Data (ICDD) is the central source for X-ray powder diffraction patterns. For metallurgical work, metals research laboratories have their own standards for alloys in a variety of conditions. Phases may be identified using a number of methods. These include visual comparison to standards, heuristic computer pattern recognition algorithms, and search/match software. The most popular method of manual search uses the *Hanawalt Manual*. This manual lists standard phases from the ICDD File along with the d spacing of their most intense reflections. The computer techniques are usually one of two approaches: those that use personal computers and search a relatively small database, and those that use large computers and access the ICDD database.

Personal Computer Program. This paper presents a third alternative for those who do not have access to large computers or who do not have their own database. The paper describes

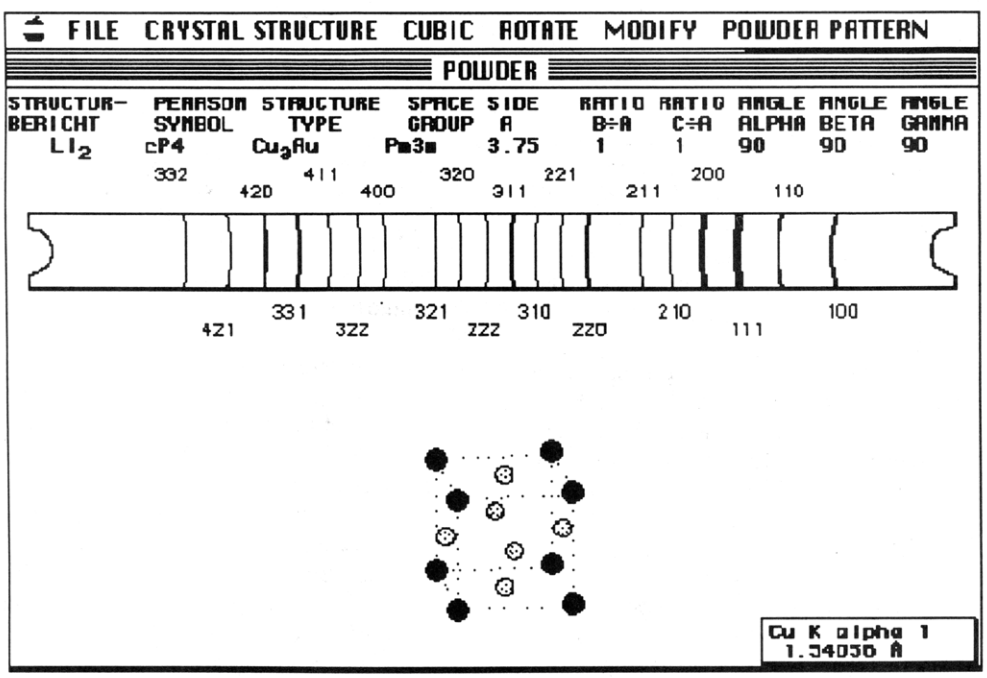

Figure 10. Mac screen print showing powder diffraction pattern of Cu_3Au.

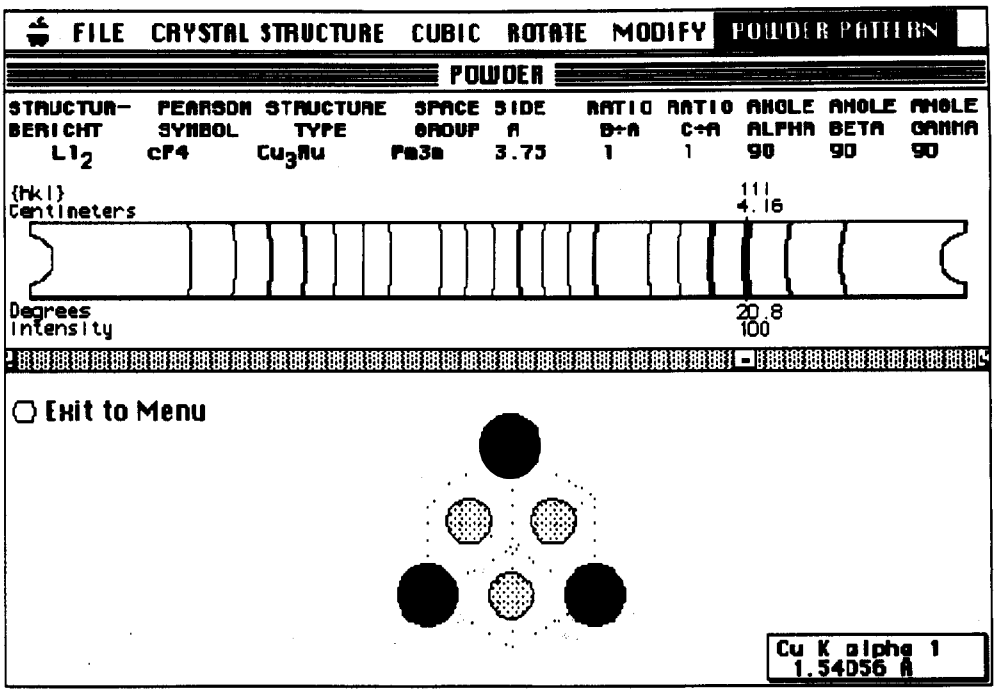

Figure 11. Mac screen print showing atoms on the {111} plane of the unit cell of an Cu_3Au crystal which causes diffraction.

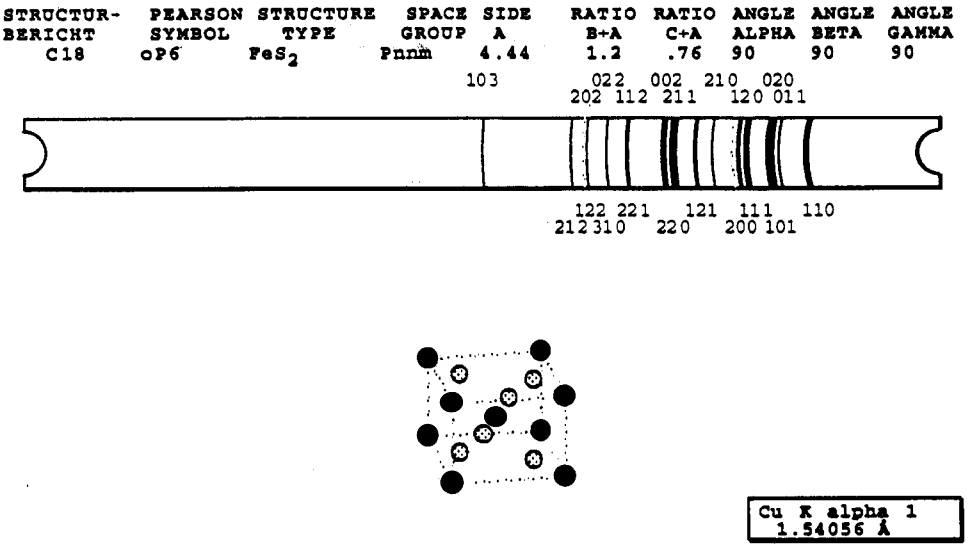

Figure 12. Simulated Debye–Scherrer powder diffraction pattern of Cu.

a program for personal computers that simulates powder patterns for cubic, tetragonal, orthorhombic, and hexagonal crystals. Phase identification is performed by comparing the pattern of the unknown with that simulated by the computer program. Because it was designed to primarily a teaching tool, the program also permits the user to obtain information which is not attainable using the other methods. The algorithm used to calculate the positions and intensities of the lines is presented in the Appendix.

The program, called POWDER, is written in two versions to run on either IBM-compatible (DOS) or Apple Macintosh (Mac) personal computers. Both versions use pull-down menus. The menus on the Mac version, of course, are implemented using the mouse, while those on the DOS version are implemented using the function (F) keys. To simulate a powder diffraction film pattern, the user may either (1) select a structure from the over 70 structure prototypes which are in the included database and modify the atomic species, dimensions of unit cell, and atomic locations or (2) open a file from the user's database. This database can be readily constructed either by saving a file constructed by modifying the prototypes provided or by entering the appropriate data. Databases constructed using DIFPAT can be read by POWDER. The database of prototypes includes Structurbericht, Pearson symbol, prototype chemical formula, and space group. This information is for convenience only and does not enter into the calculations which only require the atomic number of the atoms, their location in the unit cell, and the lengths of the crystal unit cell *a*, *b*, or *c*.

Once a structure is selected, an open model of the crystal structure is displayed on the screen. The crystal model uses the same subroutine as in DIFPAT. Consequently, this model may be rotated in real time so that the user can better visualize the structure and verify that it is the one desired. At this stage, the prototype structure, if selected, may be modified. Any changes in crystal parameters cause an update of the model on the screen.

The user may either elect to calculate a pattern using the default Cu Kα1 radiation or change the radiation. The wavelengths for the common X-ray target materials can be entered by selecting the X-ray target materials from a menu.

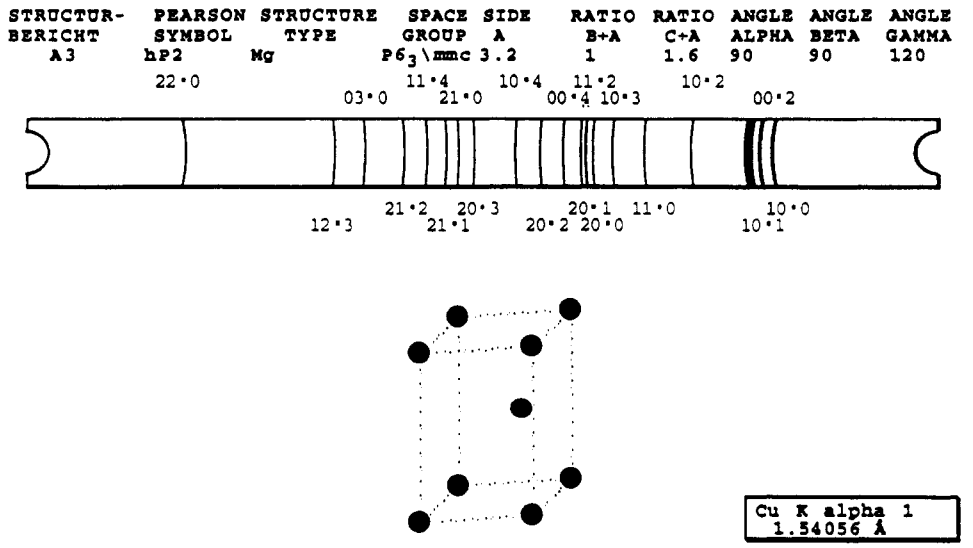

Figure 13. Simulated Debye–Scherrer powder diffraction pattern of Mg.

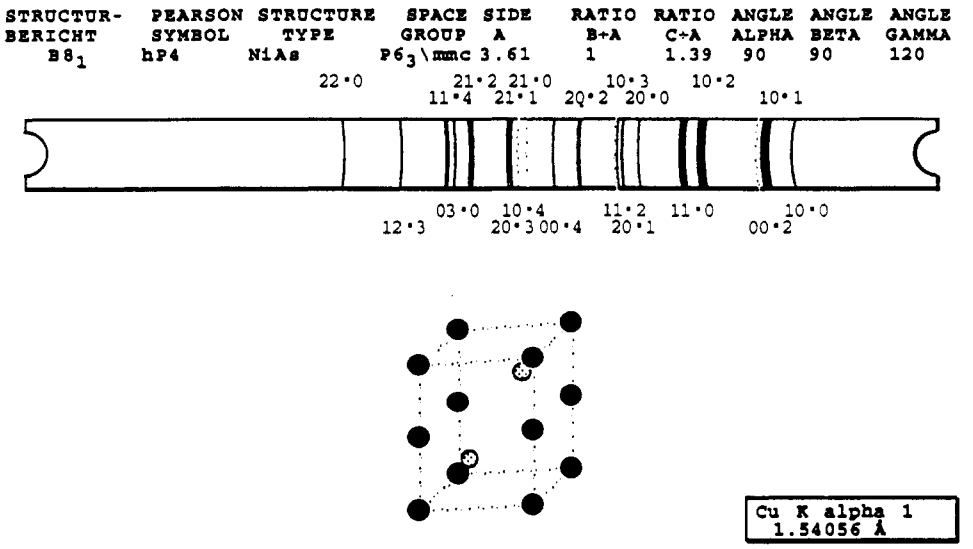

Figure 14. Simulated Debye–Scherrer powder diffraction pattern of marcasite.

Table IV. Data from POWDER Simulation of Debye–Scherrer Pattern of Cu

hkl	*d*, Å	2θ	intensity
111	2.0842	43.4	100
200	1.8050	50.5	46
220	1.2763	74.2	27
311	1.0885	90.1	34
222	1.0421	95.3	11
400	0.9025	117.2	8
331	0.8282	136.9	40
420	0.8072	145.2	49

Table V. Data from POWDER Simulation of Debye–Scherrer Pattern of Mg

hkl	*d*, Å	2θ	intensity
100	2.7713	32.3	25
002	2.5600	35.0	26
101	2.4372	36.8	100
102	1.8805	48.4	15
110	1.6000	57.6	17
103	1.4532	64.0	18
200	1.3856	67.5	2
112	1.3568	69.2	18
201	1.3375	70.3	13
004	1.2800	74.0	2
202	1.2186	78.4	3
104	1.1620	83.0	3
203	1.0757	91.5	6
210	1.0475	94.7	1
211	1.0262	97.3	11
114	0.9995	100.8	7
212	0.9694	105.2	3
105	0.9605	106.6	5
204	0.9402	110.0	2

Alternatively, numerical values for the wavelengths can be entered.

An unlabeled pattern or one which has the planes causing diffraction to be labeled adjacent to the lines may be displayed. The widths of the lines are presented in a manner to simulate the darkening on film, which is roughly proportional to the intensities of the diffracted radiation. The geometry of most Debye–Scherrer cameras is such that the camera diameter is equal in millimeters to the number of degrees in a radian, 57.3, and that the maximum value of the diffraction angle is 90°. Therefore, the film length is 180 mm, and twice the value of the diffraction angle in degrees, 2θ, equals the length along the film in millimeters. Because of the geometry, the film length is 90 mm for a Guinier camera with the same diameter, so that the angle in degrees equals the length along the film. Because of these relationships, the default length of the pattern in POWDER is set so that it is 180 mm on most screens. The standard Macintosh display uses 72 pixels per inch, so the film length is set at 510 pixels. It can be readily changed to a length of 90 mm. On PC screens, the number

Table VI. Data from POWDER Simulating a Debye–Scherrer Pattern of Marcasite FeS_2

hkl	*d*, Å	2θ	intensity
110	3.4109	26.1	59
011	2.8508	31.4	2
101	2.6866	33.3	100
020	2.6640	33.6	31
111	2.3989	37.5	42
120	2.2844	39.4	39
200	2.2200	40.6	<1
210	2.0492	44.2	5
121	1.8917	48.1	38
211	1.7515	52.2	77
220	1.7055	53.7	11
002	1.6872	54.3	27
130	1.6490	55.7	17
031	1.5716	58.7	28
221	1.5221	60.8	8
112	1.5123	61.2	9
131	1.4815	62.7	11
310	1.4260	65.4	19
022	1.4254	65.4	8

Table VII. Data from POWDER Simulation of Debye–Scherrer Pattern of NiAs

hkl	*d*, Å	2θ	intensity
100	3.1264	28.5	12
101	2.6535	33.8	100
002	2.5089	35.8	1
102	1.9568	46.4	91
110	1.8050	50.5	66
200	1.5632	59.0	1
201	1.4924	62.1	15
103	1.4748	63.0	15
112	1.4652	63.4	1
202	1.3267	71.0	23
004	1.2545	75.8	6
210	1.1817	81.4	<1
104	1.1642	82.2	1
211	1.1502	84.1	13
203	1.1421	84.8	6
212	1.0690	92.2	25
300	1.0421	95.3	11
114	1.1301	96.8	22
204	0.9784	103.9	1
213	0.9651	105.9	10

Table VIII. Data on Copper Sample Using Debye–Scherrer X-ray Powder Camera (Ref 7)

hkl	2θ	intensity
111	43.4	very strong
200	50.6	strong
220	74.2	strong
311	90.0	strong
222	95.2	medium
400	117.0	weak
331	136.8	strong
420	145.2	strong

Table IX. Data on Copper Sample Using X-ray Diffractometer (ICDD Card 4-0836)

hkl	*d*, Å	intensity
111	2.088	100
200	1.808	46
220	1.278	20
311	1.090	17
222	1.0436	5
400	0.9038	3
331	0.8293	9
420	0.803	8

Table X. Calculated Data on Copper Sample Simulating X-ray Diffractometer (Ref 9)

hkl	*d*, Å	2θ	intensity
111	2.08701	43.32	100
200	1.80740	50.45	44.9
220	1.27802	74.13	21.8
311	1.08990	89.94	23.1
222	1.04350	95.15	6.6
400	0.90370	116.94	3.8
331	0.82929	136.52	17.0
420	0.80829	144.73	19.9

Table XI. Data on Magnesium Sample Using X-ray Diffractometer (ICDD Card 35-821)

hkl	*d*, Å	intensity
100	2.778	25
002	2.605	36
101	2.452	100
102	1.9002	15
110	1.6047	12
103	1.4730	16
200	1.3899	2
112	1.3644	13
201	1.3430	8
004	1.3028	2
202	1.2264	2
104	1.1797	2
203	1.0854	3
210	1.0506	1
211	1.0299	4
114	1.0166	3
105	0.9760	2
212	0.9742	2
204	0.9505	<1
300	0.9266	1
213	0.8988	2
302	0.8729	1
205	0.8338	<1
106	0.8289	<1
214	0.8178	<1
303	0.8174	<1
220	0.8023	<1

of pixels per inch depends on the size of the monitor. The length is set for the popular 14-inch size, but may be easily adjusted for particular screens. Because of this flexibility, patterns may be readily compared by holding the film pattern near the screen. Screen prints of the cubic $L1_2$ structure Cu_3Au (Macintosh), Figure 9, and cubic NaCl structure (DOS), Figure 10, illustrate the crystal model and the simulation of the pattern. The pattern and crystal structure model can also be printed using a laser printer to provide higher resolution than a screen print.

In addition to the simulation, a table of data is displayed on request. The table presents the Miller indices of the planes causing diffraction, the relative intensities of the lines, the *d* spacing of the diffracting planes, and the values of 2θ in degrees.

The data for the pattern may also be temporarily stored in memory so that it may be used subsequently to combine with data for other material. In this way, multiphase materials may be identified. The relative intensities are adjusted according to the volume fraction present so that the intensity of the most intense reflection of the simulated dual-phase material equals 100%, but no attempt is made to simulate absorption effects.

One unique feature of POWDER is the ability to display the atomic arrangements of the atoms on specific planes of the unit cell. With this feature, the relationship between the diffraction pattern and the arrangement of atoms in the crystal becomes clearer. Figure 11 is a Mac screen print showing the atoms on the (111) plane in the unit cell of Cu_3Au that contribute to the diffracted beam. To illustrate the planes

Table XII. Calculated Data on Magnesium Sample Simulating X-ray Diffractometer (Ref 9)

hkl	*d*, Å	2θ	intensity
100	2.77951	32.18	24.3
002	2.60535	34.39	26.7
101	2.45242	36.61	100
102	1.90085	47.81	14.4
110	1.60475	57.37	15.3
103	1.47296	63.06	16.3
200	1.38975	67.32	2.1
112	1.36636	68.63	15.8
201	1.34281	70.01	11.0
004	1.30268	72.5	2.1
202	1.22621	77.83	2.5
104	1.17955	81.54	2.1
203	1.08514	90.45	4.5

Table XIII. Data on Marcasite FeS_2 Sample Using X-ray Diffractometer (ICDD Card 37-475)

hkl	*d*, Å	intensity
110	3.439	60
011	2.873	2
020	2.712	35
101	2.693	100
111	2.413	45
120	2.315	40
200	2.221	1
210	2.055	5
121	1.912	30
211	1.757	70
220	1.718	10
002	1.693	20
130	1.675	16
031	1.595	25
221	1.5325	7
112	1.5187	6
131	1.5015	9
022	1.4362	6
310	1.4288	16
230	1.4023	1
122	1.3666	12

causing diffraction of individual planes, the subroutine which produces the crystal model was modified so that the atoms above and below the plane selected are not displayed.

Comparison with Other Work. POWDER was evaluated by comparing its results with those from samples obtained by using film and/or a diffractometer and with result of a computer program which runs on a VAX minicomputer and simulates a diffractometer. All results were obtained using

Table XIV. Calculated Data on Marcasite FeS_2 Sample Simulating X-ray Diffractometer (Ref 9)

hkl	*d*, Å	2θ	intensity
110	3.41090	26.1	58.9
011	2.85076	31.3	1.9
101	2.68657	33.3	100
020	2.66400	33.6	30.7
111	2.39886	40.3	43.3
120	2.28436	36.0	39.1
200	2.22000	40.6	0.2
210	2.04923	44.1	4.3
121	1.89166	48.1	35.9
211	1.75154	52.2	68.7
220	1.70545	53.7	10.4
002	1.68720	54.3	23.9
130	1.64897	55.7	15.0
031	1.57161	58.7	23.9
221	1.52209	60.8	5.9
112	1.51230	61.2	8.2
131	1.48154	62.7	8.3
310	1.42601	65.4	15.1
022	1.42538	65.4	6.4
230	1.38682	67.5	1.2
122	1.35716	69.2	10.0

Cu Kα X-radiation. The printouts of simulated patterns for copper, magnesium, marcasite, and NiAs samples that were obtained from POWDER are presented in Figures 11–14, and data output are presented in Tables IV–VII. The results for *d* spacings and two theta do not agree exactly because the lattice parameters and atomic positions from difference sources are not in perfect agreement.

The results for the cubic copper sample (Figure 12, Table IV) can be compared with data obtained using a Debye–Scherrer camera, Table VIII, a diffractometer (ICDD card 4-0836), Table IX, and with output from a minicomputer program, Table X. Except for the intensities of the {331} and {420} planes, the results of the experiments and simulations are all in good agreement. The experiments using the film method reported equally strong reflections for the {200}, {220}, {311}, {331}, and {420} planes, and POWDER gave values that ranged from 27 to 49% of peak intensity. In contrast, the intensities of the {331} and {420} planes for the sample run on the diffractometer were about one-fifth that for the {200} plane. The minicomputer program overestimated the intensities of the higher index planes by a factor of 2.

The results of tests and simulations on the hexagonal metal magnesium, (Figure 13, Table V) are compared with the results

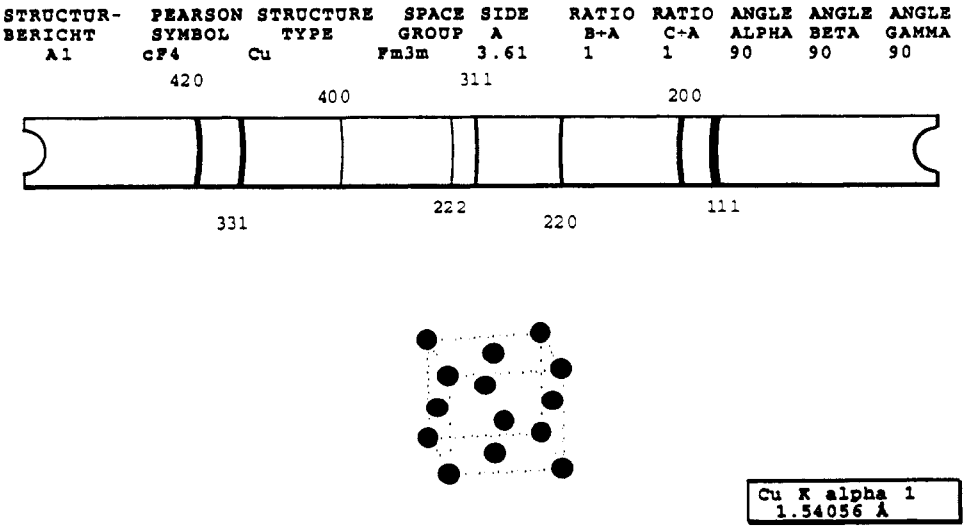

Figure 15. Simulated Debye–Scherrer powder diffraction pattern for NiAs.

Table XV. Calculated Data on NiAs Sample Simulating X-ray Diffractometer (Ref 9)

hkl	*d*, Å	2θ	intensity
100	3.12635	28.53	14.1
101	2.65348	33.75	100
002	2.50895	35.76	0.3
102	1.95676	46.37	92.9
110	1.80500	50.52	64.8
200	1.56318	59.05	1.4
201	1.49244	62.15	13.6
103	1.47482	62.97	12.9
112	1.46522	63.43	0.4
202	1.32674	70.99	20.4
004	1.25447	75.76	5.1
210	1.18165	81.37	1.6
104	1.16424	82.85	0.7
211	1.15019	84.09	9.9
203	1.14207	84.83	4.8
212	1.06902	92.20	17.7
300	1.04212	95.32	7.8
114	1.03012	96.80	15.1
204	0.97838	103.87	0.4
213	0.96511	105.91	6.1
302	0.96240	106.34	0.2
105	0.95555	107.44	3.0
220	0.90250	117.19	6.2

for a sample run using a diffractometer, Table XI, and with a minicomputer simulation of a diffractometer, Table XII. The results from POWDER were in excellent agreement.

The POWDER simulations of marcasite, an orthorhombic version of FeS_2 (Figure 14, Table VI), also agree with the results of the diffractometer experiment, Table XIII, and the minicomputer simulation, Table XIV.

The POWDER program (Figure 15, Table VII) also successfully matched the minicomputer simulation of hexagonal NiAs, Table XV, except for predictions at the higher end of the 2θ scale.

CONCLUSIONS

Programs for DOS and Macintosh personal computers have been developed that simulate electron and X-ray diffraction patterns. They can be used as an alternate to conventional methods of identifying crystalline materials and as aids in learning the principles of diffraction.

APPENDIX

Procedure To Calculate Location and Relative Intensity of Lines on POWDER Pattern. Input: Miller indices of plane (*hkl*), its multiplicity factor P_{hkl}, coordinates of atoms in unit cell (x, y, z), their atomic numbers (Z), parameters of unit cell (a, b, c), and incident radiation.

For each *hkl*:

Calculate interplanar spacing, d.

Input: a, b, c

Cubic: $1/d^2 = (h^2k^2 + l^2)/a^2$

Tetragonal: $1/d^2 = (h^2 + k^2)/a^2 + l^2/c^2$

Orthorhombic: $1/d^2 = h^2/a^2 + k^2/b^2 + l^2/c^2$

Hexagonal: $1/d^2 = 4/3[(h^2 + hk + k^2)/a^2)] + l^2/c^2$

Calculate θ.

Input: λ, d

$\theta = \arcsin(\lambda/2d)$

Calculate atomic scattering factor, f, for each atom in unit cell:

Input: $\sin\theta$, λ, Z

Linearly interpolate data from lookup table taken from Appendix 12 of Cullity (ref 7).

Calculate contribution to square of atomic scattering factor of unit cell, $|F|^2$.

Input: f, P_{hkl}, *hkl*, x,y,z

$|F|^2 = [f_1P_{hkl}\cos 2\pi(hx_1 + ky_1 + lz_1) + \ldots + f_nP_{hkl}\cos 2\pi(hx_n + ky_n + lz_n)]^2 + [f_1P_{hkl}\sin 2\pi(hx_1 + ky_1 + lz_1) + \ldots + f_nP_{hkl}\sin 2\pi(hx_n + ky_n + lz_n)]^2$

After performing calculations for each *hkl*, then:

Order values for $|F|^2$ with increasing θ, and bundle $|F|^2$ for *hkl*'s having identical θ.

Calculate intensity, I, for each θ.

$I = |F|^2[(1 + \cos^2 2\theta)/(\sin^2\theta\cos\theta)]$

Normalize intensities for each θ.

$I_n = 100\ I/I_{max}$

REFERENCES AND NOTES

(1) Edington, J. W. *Practical Electron Microscopy in Materials Science*, Van Nostrand Reinhold: New York, 1976.
(2) Loretto, M. H. *Electron Beam Analysis of Materials*; Chapman and Hall: New York, 1984.
(3) Sirotin, Yu. I.; Shaskolskaya, M. P. *Fundamental of Crystal Physics*, Mir Publishers: Moscow, 1982.
(4) Kirkland, E. J. Viewing Molecules with the Macintosh; *Byte* **1985**, 251.
(5) Grillo, J. P.; Robertson, J. D. *Data and File Management*; W. C. Brown: New York, 1983.
(6) Park, C. S. *Interactive Microcomputer Graphics*; Addison-Wesley: Reading, MA, 1985.
(7) Cullity, B. D. *Elements of X-ray Diffraction*, 2nd ed.; Addison-Wesley: Reading, MA, 1978.
(8) ICDD Cards 37-475, 35-821, and 4-0836.
(9) Smith, D. K.; Johnson, G. G.; Scheible, A. *X-ray Diffraction Powder Generation Package POWD12, VAX Version*; Materials Research Laboratory, The Pennsylvania State University: 1991; pp 2–15.